Available online at www.sciencedirect.com
ScienceDirect
Inorganica Chimica Acta 360 (2007) 529–534
Inorganica Chimica Acta
www.elsevier.com/locate/ica

A comparison of vanadyl acetylacetonate complexes of N_2O heteroscorpionate ligands that vary systematically in donor set

V. Manivannan, Justin T. Hoffman, Vincent L. Dimayuga, Timothy Dwight, Carl J. Carrano *

Department of Chemistry and Biochemistry, San Diego State University, San Diego, CA 92182-1030, USA

Received 3 July 2006; accepted 28 July 2006
Available online 10 August 2006

Abstract

We have successfully prepared a series of vanadyl complexes with N_2O heteroscorpionate ligands and have characterized their *cis* and *trans* geometrical isomers both in solution and the solid state. The major difference between the isomers, and between the various oxygen atom donors of the N_2O scorpionate ligands, is in their redox potentials which can span almost a volt for this ostensively similar set of compounds. Such data may be useful in screening vanadium complexes for potential biological activity.

Keywords: Vanadium complexes; Heteroscorpionate ligands; X-ray diffraction

1. Introduction

Vanadium complexes are increasingly important potential drug candidates for treatment of a wide range of human and animal diseases [1,2]. Perhaps most notable are the V(IV) maltol complexes which are now undergoing clinical trials as potential orally active insulin substitutes for the treatment of diabetes [3]. While the insulin mimetic chemistry of V(IV) and V(V) is an extremely exciting and robust field, metal complexes of this element also are reported to have spermicidal, apoptotic and anticancer effects as well [4–9]. Among the many V(IV) complexes examined for anticancer and insulin mimetic activity are vanadyl complexes of the acetylacetone ligand [5,10,11]. Although these complexes have been known for decades and are well characterized structurally, their solution chemistry is often complex. This coupled with the tendency of vanadium to engage in redox activity between its two major oxidation states of 4+ and 5+ has hampered the ability to determine a mechanism of action particularly with respect to their insulin mimetic properties.

One of the most powerful methods utilized by biochemists and molecular biologists in the determination of structure and mechanism of proteins is so called site directed mutagenesis. Using this approach it is possible to make single amino acid changes in a known protein and to systematically examine the results of such changes. Recently we and others have created a family of monoanionic tripodal terdentate ligands that now gives the inorganic chemist access to a somewhat similar methodology by allowing systematic changes of donor atoms while keeping other variables essentially constant [12–15]. Further generations of this ligand family have now opened up the possibility that second sphere coordination effects such as hydrogen bonding can also be explored in a systematic way.

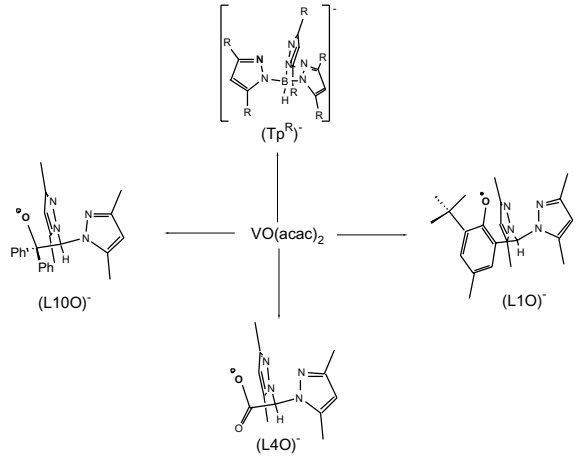

* Corresponding author. Tel.: +1 619 594 5929; fax: +1 619 594 4634.
E-mail address: carrano@sciences.sdsu.edu (C.J. Carrano).

0020-1693/$ - see front matter © 2006 Elsevier B.V. All rights reserved.
doi:10.1016/j.ica.2006.07.089

A second distinct advantage of the C_2 symmetric heteroscorpionates is the ability to probe the effects of geometrical isomerization on metal ion properties. Thus for monooxo metalates both *cis* and *trans* geometries can be defined corresponding to the orientation of the heteroatom of the scorpionate ligand with respect to the oxo group. In previous work we have isolated and characterized such isomers for monooxo Mo(V) complexes [16,17].

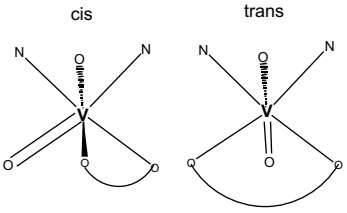

Given the importance of vanadyl(acac) species in drug research we describe here a series of complexes of the type [LVO(acac)] where the donor set provided by L varies systematically from $N_2O_{carboxylate}$ to $N_2O_{phenoxide}$ to $N_2O_{alkoxide}$. Studies such as this may make mechanistic studies on the mode of action of potential vanado-drugs more systematic.

2. Experimental

All syntheses were carried out in air and the reagents and solvents purchased from commercial sources and used as received unless otherwise noted. Methanol was distilled under argon over CaH_2, THF from sodium/benzophenone and CH_2Cl_2 from CaH_2. The ligands L1OH, Li[L4O] and L10OH were prepared as previously described as was the complex [(Tp*)VO(acac)] [18,19].

2.1. [(L1O)VO(acac)] (1)

L1OH (0.58 g, 1.58 mmol) and $VO(acac)_2$ (0.42 g, 1.58 mmol) were suspended in 20 ml of methanol and heated briefly to reflux under an Ar atmosphere. After stirring overnight the pale green solid that deposited was filtered off and washed extensively with methanol. X-ray quality crystals were obtained by slow diffusion of isopropyl ether into a solution of the crude product in dichloromethane–benzene (9:1) at −15 °C. Yield: 0.48 g (57%). *Anal*. Calc. for $C_{27}H_{36}N_4O_4V\cdot 0.83C_6H_{14}O$: C, 62.20; H, 7.28; N, 9.08. Found: C, 62.69; H, 7.37; N, 9.01%. IR(KBr, cm^{-1}) $\nu_{CO}(acac) = 1593$; $\nu_{C=N} = 1560$, 1518; $\nu_{VO} = 944$. λ_{max}, CH_2Cl_2 ($M^{-1}\,cm^{-1}$): 698 nm (33), 625 nm (32), 366 nm (1295).

2.2. [(L4O)VO(acac)] (2)

Li(L4O) (1.05 g, 4.1 mmol) and $VO(acac)_2$ (1.1 g, 4.1 mmol) were dissolved in 20 ml of methanol and heated briefly to reflux under an Ar atmosphere to produce a deep blue–green solution. After stirring overnight the solution was filtered and the solvent removed under high vacuum. The crude product was recrystallized from dichloromethane/hexane to yield X-ray quality crystals. Yield: 0.48 g (57%). *Anal*. Calc. for $C_{17}H_{21}N_4O_5V\cdot 0.5CH_2Cl_2\cdot H_2O$: C, 44.45; H, 5.12; N, 11.85. Found: C, 44.93; H, 5.13; N, 11.79%. IR (KBr, cm^{-1}) $\nu_{COO} = 1667$, $\nu_{CO}(acac) = 1579$; $\nu_{C=N} = 1559$, 1524; $\nu_{VO} = 960$. λ_{max}, CH_2Cl_2 ($M^{-1}\,cm^{-1}$): 722 nm (29), 558 nm (10), 394 nm (42).

2.3. [(L10O)VO(acac)] (3)

L10OH (0.78 g, 2.0 mmol) and $VO(acac)_2$ (0.54 g, 2.0 mmol) were dissolved in 20 ml of methanol and heated under reflux for 12 h. The resulting deep blue–green solution was filtered and the solvent removed under high vacuum. The crude product was taken up several times in dichloromethane and refiltered to remove an insoluble green precipitate. A concentrated solution was then triturated with ether and allowed to stand at −20 °C overnight, filtered and air dried. Yield: 0.35 g (32%). *Anal*. Calc. for $C_{29}H_{32}N_4O_4V\cdot 1/4H_2O$: C, 62.65; H, 5.89; N, 10.07. Found: C, 62.74; H, 6.08; N, 9.75%. IR (KBr, cm^{-1}) $\nu_{CO}(acac) = 1588$; $\nu_{C=N} = 1560$, 1518; $\nu_{VO} = 957$. λ_{max}, CH_2Cl_2: 800, 584, 399, 424(sh).

2.4. Physical methods

Elemental analyses were performed on all compounds by Numega, San Diego, CA. All samples were dried in vacuo prior to analysis. IR spectra were recorded as KBr disks on a ThermoNicolet Nexus 670 FT-IR spectrometer and are reported in wavenumbers. Cyclic voltammetric experiments were conducted using a BAS Epsilon (Bioanalytical Systems Inc., West Lafayette, IN) voltammetric analyzer. All experiments were done under argon at ambient temperature in solutions with 0.1 M tetrabutylammonium hexafluorophosphate as the supporting electrolyte. Cyclic voltammograms (CV) were obtained using a three-electrode system consisting of glassy-carbon working, platinum wire auxiliary, and SCE reference electrodes. The ferrocinium/ferrocene couple was used to monitor the reference electrode and was observed at 0.450 V with $\Delta Ep = 0.120$ V and $ip_c/ip_a \approx 1.0$ in CH_2Cl_2 under these conditions. IR compensation was applied before each CV was recorded. Potentials are reported versus the saturated calomel couple. Electronic spectra were recorded using a Cary 50 UV–Vis spectrophotometer. EPR spectra were obtained in dichloromethane solution at room temperature on a MicroNow 8300A X-band spectrometer operating at ca. 9.36 GHz. Conditions: 3400 G field center, 500 G sweep width, 1.6 G modulation amplitude, 30 s scan time.

2.5. X-ray crystallography

Crystal, data collection, and refinement parameters for **1**–**3** are given in Table 1. Crystals of all complexes were sealed in thin-walled quartz capillaries, mounted on either a Siemens P4 (data collected at 293 K), a Nonius Kappa

Table 1
Summary of crystallographic data and parameters for *trans*-[(L1O)VO(acac)]·$C_6H_{14}O$, *trans*-[(L4O)VO(acac)]·CH_2Cl_2, and *cis*-[(L10O)VO(acac)]

	1	2	3
Molecular formula	$C_{33}H_{51}N_4O_5V$	$C_{18}H_{22}N_4O_5Cl_2V$	$C_{29}H_{32}N_4O_4V$
Fw	634.71	496.24	551.53
Temperature (K)	153(2)	293(2)	293(2)
Crystal system	triclinic	monoclinic	monoclinic
Space group	$P\bar{1}$	$P2_1/c$	$C2/c$
Cell constants			
a (Å)	11.145(2)	13.212(2)	17.0123(7)
b (Å)	11.692(2)	19.253(3)	8.3088(3)
c (Å)	14.234(3)	8.975(2)	39.9775(13)
α (°)	92.81(3)	90	90
β (°)	109.89(3)	93.209(13)	99.592(2)
γ (°)	99.75(3)	90	90
Z	2	4	8
V (Å^3)	1707.5(6)	2253.9(7)	5571.9(4)
Absorption coefficient μ_{calc} (mm^{-1})	0.334	0.713	0.397
$\delta_{calc.}$ (g/cm^3)	1.233	1.462	1.315
$F(000)$	678	1020	2312
Crystal dimensions (mm)	$0.2 \times 0.4 \times 0.02$	$0.8 \times 0.8 \times 0.5$	$0.4 \times 0.2 \times 0.2$
Radiation, λ (Å)	Mo Kα (0.71073)	Mo Kα (0.71073)	Mo Kα (0.71073)
h,k,l Ranges collected	$-8 \rightarrow 8$, $-15 \rightarrow 13$, $-18 \rightarrow 17$	$-14 \rightarrow 14$, $-20 \rightarrow 0$, $0 \rightarrow 9$	$-23 \rightarrow 23$, $-11 \rightarrow 7$, $-55 \rightarrow 55$
θ Range (°)	3.0–27.46	2.12–22.51	1.03–29.52
Number of reflections collected	17732	3156	47220
Number of unique reflections	5673	2930	7746
Number of parameters	388	292	343
Data/parameter ratio	14.62	10.03	22.58
Refinement method	full-matrix least-squares of F^2	full-matrix least-squares of F^2	full-matrix least-squares of F^2
$R(F)$[a]	0.0792	0.0499	0.0587
$R_w(F^2)$[b]	0.2205	0.1340	0.1629
Goodness-of-fit w[c]	1.023	1.011	1.019
Largest difference in peak and hole (e/Å^3)	1.298 and −0.658	0.310 and −0.359	0.407 and −0.420

[a] $R = [\sum |\Delta F| / \sum |F_o|]$.
[b] $R_w = [\sum w(\Delta F)^2 / \sum wF_o^2]$.
[c] Goodness-of-fit on F^2.

Table 2
Selected bond lengths (Å) and angles (°)

	1	2	3
V–O_{oxo}	1.630(3)	1.588(3)	1.595(1)
V–O_{lig}	2.026(3)	2.128(3)	1.903(2)
V–O_{acac}	1.980(3)	1.983(3)	2.011(2)
V–O_{acac}	1.992(3)	1.979(3)	2.022(2)
V–N1	2.127(4)	2.138(3)	2.113(2)
V–N3	2.140(4)	2.141(3)	2.399(2)
O(1)–V(1)–O(4)	97.23(14)	98.93(13)	104.12(10)
O(1)–V(1)–O(3)	98.11(14)	101.16(13)	99.23(10)
O(4)–V(1)–O(3)	89.84(12)	89.28(12)	87.94(7)
O(1)–V(1)–O(2)	175.38(12)	172.07(12)	96.33(10)
O(4)–V(1)–O(2)	86.82(12)	87.21(11)	159.44(8)
O(3)–V(1)–O(2)	84.08(12)	83.83(11)	86.70(8)
O(1)–V(1)–N(1)	92.73(16)	94.82(14)	96.22(10)
O(4)–V(1)–N(1)	92.49(13)	92.08(12)	87.45(7)
O(3)–V(1)–N(1)	168.55(14)	163.55(12)	164.53(8)
O(2)–V(1)–N(1)	84.85(13)	79.87(12)	92.49(8)
O(1)–V(1)–N(3)	92.48(13)	92.80(13)	172.20(11)
O(4)–V(1)–N(3)	169.88(12)	167.82(12)	80.47(7)
O(3)–V(1)–N(3)	91.65(13)	91.66(11)	87.73(7)
O(2)–V(1)–N(3)	83.38(12)	80.82(11)	79.49(7)
N(1)–V(1)–N(3)	84.15(14)	83.64(12)	76.91(7)

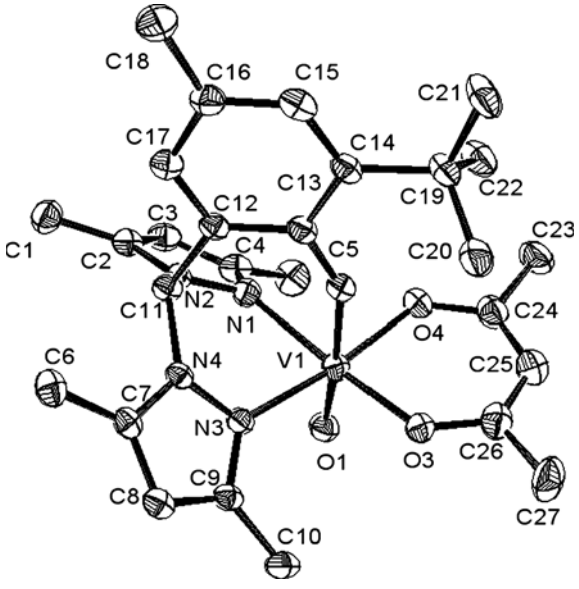

Fig. 1. Thermal ellipsoid diagram (40%) for **1** showing complete atomic labeling.

CCD (data collected at 153 K) or a Bruker X8 APEX (data collected at 293 K) diffractometer using molybdenum radiation. For the Siemens system automatic searching (Siemens XSCANS 2.1), centering, indexing, and least-squares routines were carried out for each crystal with at least 25 reflections in the range, $20° \leqslant 2\theta \leqslant 25°$ used to determine the unit cell parameters. During the data collection, the intensities of three representative reflections were measured every 97 reflection, and any decay observed was empirically corrected for by the software during data processing. We thank Dr. Vincent Lynch, Department of Chemistry University of Texas at Austin for data collection on **2**. The procedures used for data collection and processing on the Bruker X8 APEX were as previously described [15,16]. The structures were all solved using direct methods or via the Patterson function, completed by subsequent difference Fourier syntheses, and refined by full-matrix least-squares procedures on F^2. All non-hydrogen atoms were refined with anisotropic displacement coefficients with hydrogens treated as idealized contributions using a riding model except were noted. All software and sources of the scattering factors are contained in the SHELXTL 5.0 program library (G. Sheldrick, Siemens XRD, Madison WI). Data collection parameters are found in Table 1 and selected bond distances and angles for these complexes are shown in Table 2. Figs. 1–3 contain the thermal ellipsoid diagrams of the three complexes.

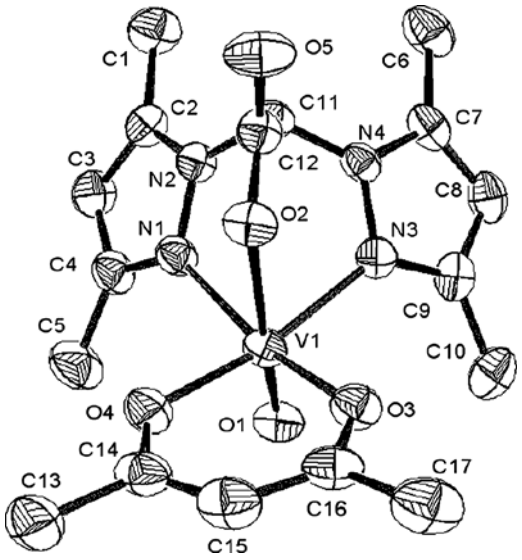

Fig. 2. Thermal ellipsoid diagram (40%) for **2** showing complete atomic labeling.

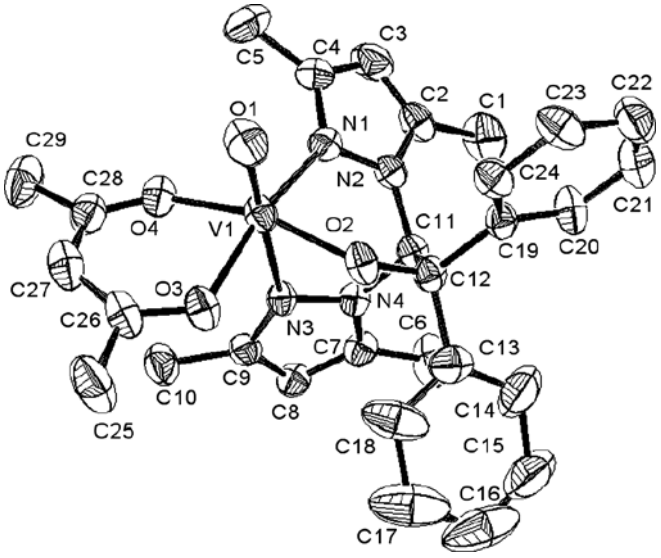

Fig. 3. Thermal ellipsoid diagram (40%) for **3** showing complete atomic labeling.

3. Results and discussion

3.1. Solid state structures

Compounds **1** and **2** both crystallized as solvates, **1** with a well-ordered isopropyl ether and **2** with a disordered dichloromethane. Both revealed a *trans* geometry with the vanadyl oxo group *trans* to the phenolate or carboxylate oxygen of the heteroscorpionate ligand respectively. The "equatorial" plane is made up of the two pyrazole nitrogens and the two oxygens of the coordinated acac. In contrast **3** was unsolvated and crystallized as the *cis* isomer where the oxo group is *trans* to a pyrazole nitrogen and the equatorial plane is made up of the two oxygens of the acac as well as the alkoxy oxygen and a pyrazole nitrogen of the scorpionate. A metrical comparison of the three structures is displayed in Table 2. The V=O bond length appears to be insensitive the nature of the group *trans* to it since the two *trans* isomers have bond lengths that bracket that found for the *cis* isomer seen in **3**. The only major structural difference between the isomers is the very long V–N bond (2.4 Å) seen for the pyrazole that is *trans* to the oxo group in **3**. This bond, which is nearly 0.3 Å longer than a "normal" V–N bond, is the result of the expected *trans* effect of the oxo group. In contrast the phenolate and carboxylate oxygens exhibit considerably smaller *trans* lengthening with the phenolate only some 0.08 Å longer than a *cis* oriented phenolate found in other V(IV)O complexes such as $VO(EHPG)^-$ [20]. The *trans* oriented carboxylate in **2** is 0.12 Å longer than the *cis* oriented carboxylate found in $VO(EHPG)^-$ but 0.16 Å shorter than the *trans* carboxylate seen in $VO(EHGS)^-$. The smaller than expected *trans* effect for the carboxylate oxygen in **2** may be the result of the more rigid ligand environment seen with the heteroscorpionates as compared to EHPG or EHGS.

3.2. Synthesis and characterization

All the complexes were prepared in the same way, that is, via proton transfer from the heteroscorpionate to vanadyl bis(acetlyacetonate) leading to facile ligand exchange and formation of [LVO(acac)]. A comparison of the phys-

Table 3
Physiochemical properties of complexes **1**–**3**

	Tp*	L1O	L4O	L10O
g_o	1.971	1.986 (*trans*) 1.953 (*cis*)	1.991	Nd
A_o (G)	101	105 (*trans*) 101 (*cis*)	100	95
E^o (V)	+1.11	+0.540 (*cis*) +0.730 (*trans*)	+1.261	+0.245
I (cm^{-1})	12903	14327	13850	12500
II	17857	16000	17921	17123
III	24875	27322	25381	24000
$\nu_{V=O}$ (cm^{-1})		954 (*cis*) 944 (*trans*)	963	957

iochemical properties of the three complexes is shown in Table 3. Compounds **1**–**3** all exhibit eight line isotropic EPR spectra in dichloromethane indicating the presence of a d^1 V(IV) (nearly 100% $I = 7/2$) nucleus. As expected, since each complex has the same N_2O_4 donor sphere dominated by the axial oxo group, the isotropic g_o and A_o values are all similar to each other. The visible spectra of all three complexes contain three more or less distinct bands in the range of 350–800 nm consistent with the Ballhausen and Grey assignments [19].

Although more labile than the corresponding second row Mo(V) complexes, we have never the less been able to characterize *cis* and *trans* geometrical isomers of these vanadyl complexes both in the solid state and in solution. Compound **2** appears only to adopt the *trans* geometry both in solution and in the solid state, analogous to the situation seen for [(L4O)$MoOCl_2$] while **3** adopts exclusively the *cis* which is contrast to the Mo(V) complex where the *trans* is the most stable isomer. Compound **1**, the sterically restrictive phenolate, clearly exists as an equilibrium mixture of both *cis* and *trans* isomers in solution. Although the crystals as isolated reveal only the *trans* isomer in the solid state, there is evidence that the *cis* isomer can also be isolated.

3.3. Electrochemistry

All the complexes reported showed quasireversible oxidative waves for the V(IV)/V(V) couple via cyclic voltammetry. Redox potentials for the three complexes span almost a volt and range from +1260 mV for **2** to +245 mV for **3**. The carboxylate complex is by far the most difficult to oxidize and its redox potential is near that found for the analogous homoscorpionate, Tp* complex with all nitrogen donors while the phenolate and the alkoxide complexes more strongly stabilize the higher valent V(V) state leading to lower redox potentials. While only a single isomer is evident for **2** and **3**, compound **1** clearly shows the existence of two species in solution with two waves of similar height observed at +540 and +730 mV in acetonitrile and at +680 and +470 in dichloromethane (Fig. 4). We assign the wave at +540 mV as the *cis* isomer and that at +730 as the *trans* based on our experience with the corresponding monooxo Mo(V) complexes. The difference in redox potential between the *cis* and *trans* isomers of 190 mV is virtually identical to the difference seen in *cis*/*trans* [(L1O)$MoOCl_2$] [16,17].

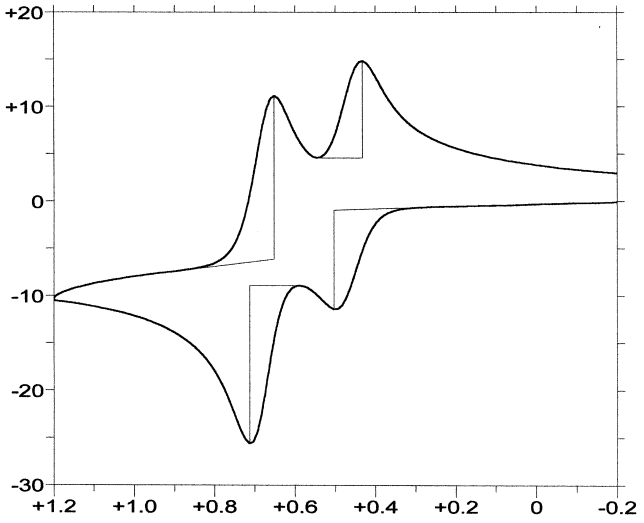

Fig. 4. Cyclic voltammogram of **1** in dichloromethane at a scan rate of 50 mV/s. Current is in μA. Other conditions as described in the text.

Controlled potential electrolysis of a pale blue/green solution of **1** in acetonitrile on a carbon basket electrode at a potential of +900 mV removed 1.09 electrons per mole confirming the one electron nature of the redox process. The final deep blue solution was EPR inactive and displayed intense peaks at 305, 360 and 770 nm in the UV–Vis spectrum characteristic of the LMCT bands seen in other monooxo V(V) phenolates and acac's [19]. The same results are seen when the controlled potential electrolysis is performed at +650 mV rather than +900 mV indicating that the *cis* and *trans* isomers are in fast equilibrium in solution. Interestingly after electrolysis a cyclic voltammogram shows only a single reversible wave at +540 mV that corresponds to the *cis* isomer. Continued potential cycling through the +540 wave or pausing the potential at +200 mV and then continuing the scan in a positive direction reveals the formation of a new "product" wave at +730 mV (Fig. 5). Re-reduction of the oxidized solution also consumes 0.983 electron and both waves are again present with approximately equal current. This behavior is consistent with an ECE mechanism due to an oxidation state dependant isomerization. Thus upon oxidation of [(L1O)VO(acac)] the resulting $[(L1O)VO(acac)]^+$ strongly favors the *cis* geometry and if the scan rate is fast only a single wave consistent with that assigned to the *cis* isomer is seen. However slowing scan rate or poising the potential for a few moments at +200 mV allows the resulting V(IV) complex to isomerize back to a mixture of *cis* and *trans* isomers and so on reversing the scan the wave due to the *trans* isomer at +730 mV appears. Similar behavior has been previously observed for some Co and Fe heteroscorpionate complexes [21].

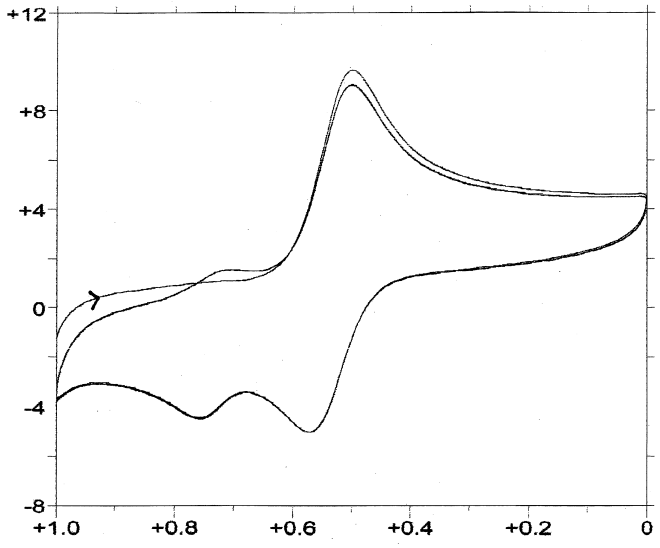

Fig. 5. Cyclic voltammogram of **1** after exhaustive electrolysis at +900 mV in acetonitrile solution. Scan direction shown by the arrow and current is in μA.

4. Conclusions

We have successfully prepared a series of vanadyl complexes with N_2O heteroscorpionate ligands and have characterized their *cis* and *trans* geometrical isomers both in solution and the solid state. The major difference between the isomers and between the various oxygen atom donors of the N_2O scorpionate ligands is in their redox potentials which can span almost a volt for this ostensively similar set of compounds. Such data may be useful in screening vanadium complexes for potential biological activity.

Acknowledgements

This work was supported in part by Grant CHE-0313865 from the NSF. The NSF-MRI program Grant CHE-0320848 is acknowledged for support of the X-ray diffraction facilities at San Diego State University. Dr. Vincent Lynch, Department of Chemistry and Biochemistry, University of Texas at Austin is gratefully acknowledged for X-ray data collection on **1**.

Appendix A. Supplementary material

Additional crystallographic data for **1**–**3** are on deposit with the Cambridge Structural Database under accession numbers CCDC 614364–614366, respectively. Supplementary data associated with this article can be found, in the online version, at doi:10.1016/j.ica.2006.07.089.

References

[1] K. Kustin, T. Tiss (Ed.), Pure Appl. Chem. 77 (2005) 1497–1654.
[2] D.C. Crans, J.J. Smee, E. Gaidamauskas, L.Q. Yang, Chem. Rev. 104 (2004) 849.
[3] K.H. Thompson, C.A. Barta, C. Orvig, Chem. Soc. Rev. 35 (2006) 545.
[4] H. Koepf, P. Koepf-Maier, Struct. Bonding (Berlin, Germany) (1988) 103.
[5] P. Ghosh, S. Ghosh, C. Navara, R.K. Narla, A. Benyumov, F.M. Uckun, J. Inorg. Biochem. 84 (2001) 241.
[6] P. Ghosh, O.J. D'Cruz, R.K. Narla, F.M. Uckun, Clin. Cancer Res. 6 (2000) 1536.
[7] P. Ghosh, O.J. D'Cruz, D.D. DuMez, J. Peitersen, F.M. Uckun, J. Inorg. Biochem. 75 (2) (1999) 135.
[8] P. Ghosh, S. Ghosh, O.J. D'Cruz, F.M. Uckun, J. Inorg. Biochem. 72 (1998) 89.
[9] R.K. Narla, Y.H. Dong, P. Ghosh, K. Thoen, F.M. Uckun, Drugs Future 25 (2000) 1053.
[10] A.T. Kotchevar, P. Ghosh, D.D. DuMez, F.M. Uckun, J. Inorg. Biochem. 83 (2001) 151.
[11] (a) S.S. Amin, K. Cryer, B. Zhang, S.K. Dutta, S.S. Eaton, O.P. Anderson, S.M. Miller, B.A. Reul, S.M. Brichard, D.C. Crans, Inorg. Chem. 39 (2000) 406;
(b) D.C. Crans, J. Inorg. Biochem. 80 (2000) 123.
[12] B.S. Hammes, C.J. Carrano, Inorg. Chem. 38 (1999) 666.
[13] B.S. Hammes, C.J. Carrano, J. Chem. Soc., Dalton Trans. (2000) 3304.
[14] A. Otero, J. Fernandez-Baeza, A. Antinolo, J. Tejeda, A. Lara-Sanchez, J. Chem. Soc., Dalton Trans. (2004) 1499.
[15] J.T. Hoffman, S. Einwächter, B.S. Chohan, P. Basu, C.J. Carrano, Inorg. Chem. 43 (2004) 7573.
[16] B.W. Kail, V.N. Nemykin, S.R. Davie, C.J. Carrano, B.S. Hammes, P. Basu, Inorg. Chem. 41 (2002) 1281.
[17] C.J. Carrano, B.S. Chohan, B.S. Hammes, B.W. Kail, V.N. Nemykin, P. Basu, Inorg. Chem. 42 (2003) 5999.
[18] J.T. Hoffman, B.L. Tran, C.J. Carrano, Dalton Trans. (2006) 3822.
[19] M. Mohan, S.M. Holmes, R.J. Butcher, J.P. Jasinski, C.J. Carrano, Inorg. Chem. 31 (1992) 2029.
[20] P.E. Riley, V.L. Pecoraro, C.J. Carrano, J.A. Bonadies, K.N. Raymond, Inorg. Chem. 25 (1986) 154.
[21] T.C. Higgs, D. Ji, R.S. Czernuscewicz, C.J. Carrano, Inorg. Chim. Acta 286 (1999) 80.